

CSIRO Publishing

# Publications of the Astronomical Society of Australia

VOLUME 18, 2001

© ASTRONOMICAL SOCIETY OF AUSTRALIA 2001

*An international journal of  
astronomy and astrophysics*



**For editorial enquiries and manuscripts, please contact:**

The Editor, PASA,  
ATNF, CSIRO,  
PO Box 76,  
Epping, NSW 1710, Australia  
Telephone: +61 2 9372 4590  
Fax: +61 2 9372 4310  
Email: Michelle.Storey@atnf.csiro.au



**CSIRO**  
PUBLISHING

**For general enquiries and subscriptions, please contact:**

CSIRO Publishing  
PO Box 1139 (150 Oxford St)  
Collingwood, Vic. 3066, Australia  
Telephone: +61 3 9662 7666  
Fax: +61 3 9662 7555  
Email: pasa@publish.csiro.au

Published by CSIRO Publishing  
for the Astronomical Society of Australia

[www.publish.csiro.au/journals/pasa](http://www.publish.csiro.au/journals/pasa)

# Shock Drift Acceleration of Electrons

Lewis Ball and D. B. Melrose

RCFTA, School of Physics, University of Sydney, NSW 2006, Australia  
ball@physics.usyd.edu.au

Received 2001 March 14, accepted 2001 September 11

**Abstract:** We review the theory of shock drift acceleration, developing the theory in detail for gyrophase-averaged particles. It is shown how both the upstream and downstream velocity spaces separate into different regions according to the interaction of the particles with the shock (reflection, transmission, head-on, overtaking). The effects of the cross-shock electric field and of the magnetic overshoot are discussed. The effectiveness of acceleration is estimated for Maxwellian and power law distributions. The condition for a beam instability to be generated by reflected particles is determined and found to be independent of the distribution function for isotropic inflowing electrons.

**Keywords:** acceleration of particles — shocks

## 1 Introduction

Charged test particles which encounter a compressive, collisionless shock can be accelerated via a process known as ‘shock drift acceleration’. The acceleration occurs because the particle’s orbit in the electric and magnetic fields at the shock results in an overall drift (after averaging over gyromotion) which converts electric potential energy to kinetic energy (e.g. Sonnerup 1969; Terasawa 1979; Toptyghin 1980, 1985; Pesses 1981; Pesses, Decker, & Armstrong 1982; Drury 1983; Armstrong, Pesses, & Decker 1985; Decker 1988). The earlier discussions of shock drift acceleration emphasised acceleration of ions, whose gyroradii are large compared with the thickness of the collisionless shock. The analogous acceleration of electrons, whose gyroradii are small compared with the thickness of the collisionless shock, is sometimes called ‘mirror reflection’. We ignore the distinction here and refer to both cases as shock drift acceleration. The acceleration is most effective at perpendicular and quasi-perpendicular shocks, and is absent in the limit of a parallel shock. (‘Perpendicular’ and ‘parallel’ refer to the orientation of the magnetic field upstream to the normal to the shock front.) The energy increase is greatest for particles which are reflected, and a fractionally large energy increase is restricted to a narrow range of initial conditions. Particles which are transmitted through the shock can also gain energy.

Shock drift acceleration of electrons is known to occur at bow shocks and interplanetary shocks, which can be studied in situ using spacecraft with instruments that can measure the field structures, wave fields, and the particle distributions (e.g. Armstrong & Krimigis 1976; Potter 1981; Sarris & Krimigis 1985; Lopate 1989). A characteristic feature of such accelerated electrons is a beam-like structure, which involves localisation in velocity space not only in the beam direction, but also in beam speed, with a gap between the speeds of thermal electrons and the beam particles. The beams are formed by a combination

of shock drift acceleration and a time-of-flight effect, associated with the reflected particles being swept back into the shock: slower particles are swept back after propagating a shorter distance than faster particles (Filbert & Kellogg 1979; Cairns 1986, 1987; Fitzenreiter, Scudder, & Klimas 1990). Shock drift acceleration of electrons may also be responsible for the acceleration of electrons which produce Type II solar radio bursts and the associated herringbone structures (Holman & Pesses 1983; Leroy & Mangeney 1984; Wu 1984; Street, Ball, & Melrose 1994; Krauss-Varban & Wu 1989) although a detailed model has yet to be developed. A more problematic possibility is that shock drift acceleration may operate as a pre-acceleration mechanism for diffusive acceleration, boosting electrons to the threshold energies thought to be required for resonant scattering to be effective (Zank & Gaisser 1992; Melrose 1994).

In Section 2 we discuss specific frames of reference which are useful for calculations involving shock drift acceleration. A useful dynamical invariant is discussed in Section 3 and a justification of the associated conservation law is presented. In Section 4 we discuss the conditions which determine whether particles incident on a shock of zero thickness are transmitted through the shock or reflected from it. The maximum energy experienced by particles which encounter a zero-thickness shock is presented in Section 5. In Section 6 the effect of structure within the shock front is discussed, with particular attention on the effects of a cross-shock electric potential difference.

## 2 Shock Frames

A shock frame is a frame of reference in which the shock is at rest. In the ‘normal incidence frame’ (NIF), also known as the ‘shock normal frame’, the fluid in the ‘upstream’ region (which has yet to encounter the shock) moves at velocity  $\mathbf{u}_1$  along the normal to the shock front as shown in the left panel of Figure 1. We use the subscripts 1 and 2

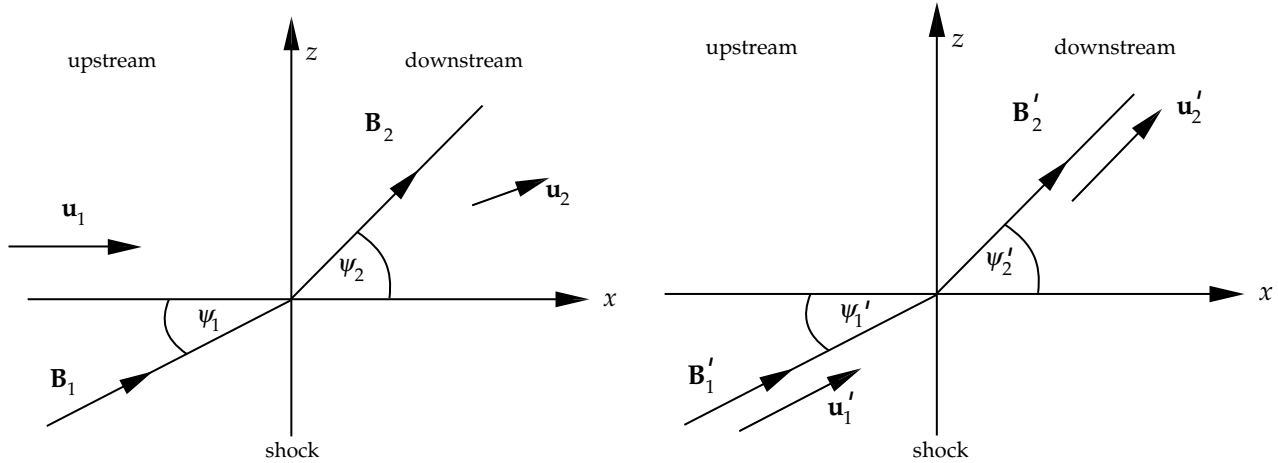


**Figure 1** Left: The normal incidence frame, in which the shock is at rest and the upstream (unshocked) fluid flows toward the shock along the shock normal. Right: The de Hoffmann–Teller frame, in which the fluid velocities are parallel to the magnetic fields on either side of the shock.

to denote parameters upstream and downstream of the shock respectively. In general the upstream magnetic field  $\mathbf{B}_1$  is at an angle  $\psi_1$  to the shock normal, the downstream field  $\mathbf{B}_2$  is at an angle  $\psi_2$ , and the fluid flow is deflected at the shock and has a velocity  $\mathbf{u}_2$  downstream of the shock.

It is useful to categorise shocks according to the speed (in the plane of the shock) of the point of intersection between a particular magnetic field line and the shock front. A shock is ‘subluminal’ if this speed is less than  $c$ , and ‘superluminal’ if it is greater than  $c$ .

If the shock is subluminal it is possible to make a Lorentz transformation to a frame in which this point of intersection is at rest, shown in the right panel of Figure 1. The existence of this frame was first pointed out by de Hoffmann & Teller (1950), and so it is often called the *de Hoffmann–Teller* frame (dHTF). We use primes to denote quantities in the dHTF. In the dHTF the fluid velocity  $\mathbf{u}'$  is parallel to the field lines on both sides of the shock. If this were not so the plasma motion perpendicular to the magnetic field would imply a motion of the magnetic field at the shock front (since a highly conducting plasma drags the field lines with it), contrary to the assumed properties of the frame. If the shock front is a simple discontinuity in the plasma properties and has negligible thickness, then since  $\mathbf{u} \parallel \mathbf{B}$  and  $\mathbf{E}' = -\mathbf{u}' \times \mathbf{B}'$ , there is no electric field in the dHTF. In the absence of an electric field, the energy of a particle — and hence the magnitude of its momentum — is conserved regardless of whether it crosses the shock or is reflected from it.

If the shock is superluminal it is possible to make a Lorentz transformation to a frame in which the shock is strictly perpendicular, i.e.  $\psi_1 = \pi/2$ . In such a frame the field lines convect perpendicularly across the shock, and the particles — which are tied to the field lines — therefore cannot be reflected. The electric field implied by  $\mathbf{E} = -\mathbf{u} \times \mathbf{B}$  is normal to the magnetic field, so that the parallel momentum is unchanged as particles cross the shock:  $p_{\parallel 1} = p_{\parallel 2}$ .

The thickness of a collisionless shock is comparable to the gyroradius of the bulk of the ions in the plasma. Energetic ions have larger gyroradii and see the shock essentially as a simple discontinuity, but the smaller gyroradii of electrons means that they are sensitive to field structure within the shock itself. In Sections 4 and 5 we treat the shock as a simple discontinuity and ignore the effects of field structures within the shock. In Section 6 we discuss the effects of two such features, the cross shock electric potential and the magnetic overshoot.

### 3 A Conservation Law

Analytical treatments of particle encounters with a shock front follow from the fact that the quantity  $p^2 \sin^2 \alpha / B$  is essentially unchanged by the encounter, where  $p$  is the particle momentum,  $B$  is the magnetic field, and  $\alpha$  is the pitch angle — the angle between  $\mathbf{p}$  and  $\mathbf{B}$ . The conservation of  $p^2 \sin^2 \alpha / B$  is equivalent to the conservation of the first adiabatic invariant, but the result has quite a different justification in this context where it applies only after averaging over gyrophase and was originally identified from numerical orbit calculations (e.g. Pesses 1981). A theoretical justification for the conservation law at a subluminal shock may be expressed in terms of Liouville’s theorem (Drury 1983).

Conservation of an infinitesimal extension in phase space in the dHTF implies

$$d^3 \mathbf{p}'_1 d^3 \mathbf{x}'_1 = d^3 \mathbf{p}'_2 d^3 \mathbf{x}'_2. \quad (1)$$

Let the shock normal be along the  $x$  axis, so that the surface areas  $dy_1 dz_1 = dy_2 dz_2$  are identically equal. Writing  $d^3 \mathbf{p}'_{1,2} = p'^2_{1,2} dp'_{1,2} d\cos\alpha'_{1,2} d\phi'_{1,2}$ , with  $p'_1 = p'_2 = p'$  and  $\phi'$  the gyrophase, (1) reduces to  $d\cos\alpha'_1 d\phi'_1 dx_1 = d\cos\alpha'_2 d\phi'_2 dx_2$ . The magnetic field is at an angle  $\psi_{1,2}$  to the shock normal, cf. Figure 1, so the velocity component along the  $x$ -axis implies  $dx_{1,2} = v' \cos\alpha'_{1,2} \cos\psi_{1,2} dt$ . Finally, the component of the magnetic field along

the shock normal is equal on either side of the shock:  $B_2 \cos \psi_2 = B_1 \cos \psi_1$ . Hence (1) reduces to

$$\frac{\cos \alpha'_1 d \cos \alpha'_1 d \phi'_1}{B_1} = \frac{\cos \alpha'_2 d \cos \alpha'_2 d \phi_2}{B_2}. \quad (2)$$

Assuming that the particle distribution is independent of gyrophase, one may integrate over gyrophase using  $\int d\phi'_{1,2} = 2\pi$ . Then (2) integrates to  $(\cos^2 \alpha' + \text{constant})/B$ , having the same value on either side of the shock. The constant of integration can be evaluated by noting that a particle with zero pitch angle on one side of the shock has zero pitch angle on the other side of the shock, that is,  $\alpha'_1 = 0 \Rightarrow \alpha'_2 = 0$ . It follows that  $\sin^2 \alpha'_1/B_1 = \sin^2 \alpha'_2/B_2$ , which establishes the result for subluminal shocks.

In the superluminal case one may choose a frame in which the shock is strictly perpendicular and no particle can be reflected. The volume elements are related by the compression ratio,  $r$ , of the shock so that  $d^3 \mathbf{x}_1 = r d^3 \mathbf{x}_2$ , as are the magnetic fields related by  $B_2 = r B_1$ . Writing  $d^3 \mathbf{p}_{1,2} = p_{\perp 1,2} dp_{\perp 1,2} dp_{\parallel 1,2} d\phi_{1,2}$ , and assuming that the distribution is independent of gyrophase, (1) reduces to  $p_{\perp 2} dp_{\perp 2} = r p_{\perp 1} dp_{\perp 1}$ , which with  $r = B_2/B_1$  integrates to give  $p_{\perp 2}^2/B_2 = p_{\perp 1}^2/B_1$ , establishing the conservation law for the superluminal case. In deriving this result we assume that the electric field is normal to the shock and to the magnetic field, so that one has  $dp_{\parallel 1} = dp_{\parallel 2}$ .

For the remainder of this work we restrict our attention to subluminal shocks, and generally assume that the transformation from the NIF to the dHTF is nonrelativistic.

#### 4 Reflection or Transmission

A single particle that encounters a subluminal shock may either cross it or be reflected, as shown in Figure 2, depending on its pitch angle. The treatment of the encounter is facilitated by making a Lorentz transformation to the dHTF and then using the conservation of  $p^2 \sin^2 \alpha/B$ .

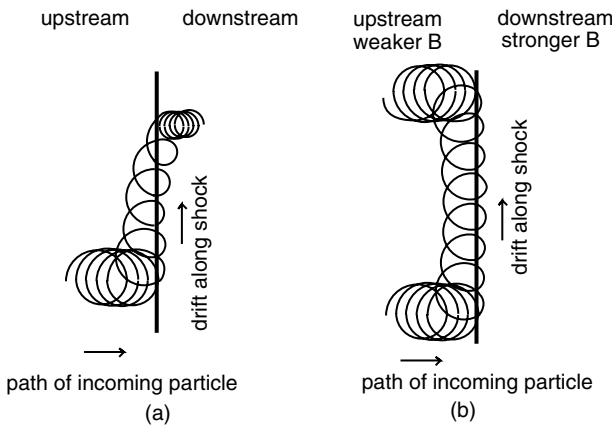


**Figure 2** A schematic charged particle orbit as it (a) crosses or (b) is reflected at a shock whose thickness is much less than the particle gyroradius. The increase in magnetic field across the shock means that the gyroradius is smaller in the downstream region than on the upstream side. The result is a particle drift along the shock that is analogous to the drift caused by a gradient in magnetic field.

When the transformation between the NIF and the dHTF is nonrelativistic the magnetic fields in the NIF and the dHTF are approximately the same, as are the angles  $\psi$ . We consider only this case below, and therefore drop the primes from these quantities.

The condition for particles to be reflected at a simple shock of zero thickness follows quite straightforwardly (e.g. Topyghin 1980, 1985). Since there is no electric field in the dHTF, and since stationary magnetic fields do no work,  $p'_2 = p'_1$ . Together with the result

$$\frac{p_2'^2 \sin^2 \alpha'_2}{B_2} = \frac{p_1'^2 \sin^2 \alpha'_1}{B_1} \quad (3)$$

this implies  $\sin^2 \alpha'_2 = (B_2/B_1) \sin^2 \alpha'_1$ . For a compressive shock,  $B_2 > B_1$ . It follows that if a particle with a pitch angle in the upstream region satisfying  $\sin^2 \alpha'_1 > B_1/B_2$  were transmitted through the shock, it would have a pitch angle in the downstream region such that  $\sin^2 \alpha'_2 > 1$ . This is of course impossible, and so such particles must be reflected rather than transmitted. Hence the condition for reflection is

$$\alpha'_1 > \alpha_c \quad \text{where} \quad \sin^2 \alpha_c = B_1/B_2. \quad (4)$$

The velocity difference between the NIF and the dHTF is in the plane of the shock and is such that  $\mathbf{u}'_1$ , with components  $u'_1 \sin \psi_1$  along the face of the shock and  $u'_1 \cos \psi_1$  normal to the shock, is transformed into  $\mathbf{u}_1$ , which is normal to the shock. Thus  $u_1 = u'_1 \cos \psi_1$ , and in the nonrelativistic case the transformation velocity is  $u_0 = u'_1 \sin \psi_1$ . Together these imply  $u_0 = u_1 \tan \psi_1$  (e.g. Webb, Axford, & Terasawa 1983; Kirk & Heavens 1989).

For a shock which is close to perpendicular with  $\psi_1 \sim 90^\circ$ , the pitch angles in the upstream plasma, in the dHTF ( $\alpha'$ ) and in the NIF ( $\alpha$ ), are related by

$$p' \cos \alpha' = p \cos \alpha + m u_0, \quad p' \sin \alpha' = p \sin \alpha, \quad (5)$$

and these imply

$$\cos \alpha' = \frac{\cos \alpha + u_1 \tan \psi_1 / v}{\left[ 1 + \frac{2u_1 \tan \psi_1}{v} \cos \alpha + \left( \frac{u_1 \tan \psi_1}{v} \right)^2 \right]^{1/2}}. \quad (6)$$

Solving for  $\cos \alpha$  gives

$$\cos \alpha = \pm \cos \alpha' \left[ 1 - \left( \frac{u_1 \tan \psi_1}{v} \right)^2 \sin^2 \alpha' \right]^{1/2} - \frac{u_1 \tan \psi_1}{v} \sin^2 \alpha'. \quad (7)$$

For  $v > u_1 \tan \psi_1$  only the positive sign is allowed, and for  $v < u_1 \tan \psi_1$  both signs are allowed. Positive and negative  $\cos \alpha$  are to be interpreted in terms of incidence from upstream and downstream (regions 1 and 2), respectively.

While equation (4) correctly describes the range of pitch angles in the dHTF for which particles will be reflected at the shock, there is an additional constraint

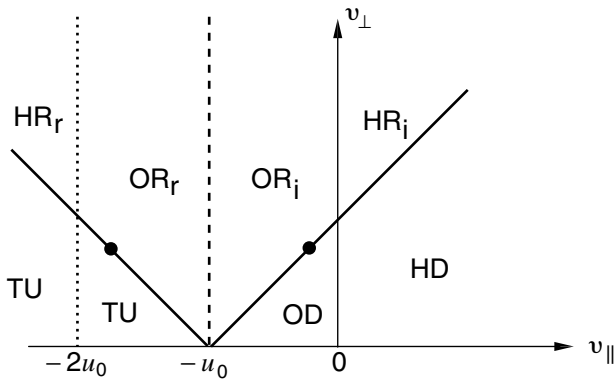


**Figure 3** Schematic of the upstream  $v$ -space in the NIF. The points corresponding to maximum energy gain are indicated by the large dots. Other labels are explained in the text.

on the pitch angles  $\alpha'_1$  which particles can have in the dHTF. Specifically, although all pitch angles are possible in the NIF, under some circumstances a range of pitch angles in the dHTF is excluded. In particular, particles with  $v > u_1 \tan \psi_1$  map to all possible values of  $\alpha'_1$  between 0 and  $2\pi$ . However, particles with  $v < u_1 \tan \psi_1$  only map to pitch angles in the dHTF which satisfy

$$\sin \alpha'_1 < v/u_1 \tan \psi_1. \quad (8)$$

On comparison of equations (4) and (8) one concludes that reflection is possible only for particles with

$$v > u_1 \tan \psi_1 (B_1/B_2)^{1/2}. \quad (9)$$

All particles for which the inequality (9) is reversed are transmitted through the shock into the downstream region.

#### 4.1 The Upstream Velocity Space

A schematic plot of the (2-dimensional) upstream velocity space in the NIF is shown in Figure 3. The different lines divide the phase space into regions based on the nature of the particles' encounter with the shock. The solid lines correspond to the reflection condition (4). The electric drift causes a particle with  $\mu = \cos \alpha_1 = 0$  to drift toward the shock with speed  $u_0$ . Hence particles with  $v_{\parallel} > -u_0$  encounter the shock. The particles that satisfy this condition and are above the diagonal line to the right are reflected from the shock. After reflection these particles appear to the left of the vertical dashed line  $v_{\parallel} = -u_0$  and above the diagonal line to the left. Particles to the right of the line  $v_{\parallel} = -u_0$  and below the diagonal line to the right encounter the shock and are transmitted downstream. Particles may also overtake the shock from the downstream region. Particles to the left of the vertical dashed line  $v_{\parallel} = -u_0$  and below the diagonal line to the left have been transmitted from downstream. The labels in Figure 3 correspond to overtaken particles that are transmitted downstream (OD), particles that encounter the shock head-on and are transmitted downstream (HD), particles that are overtaken by the shock and are reflected upstream (OR), particles that encounter the shock head-on and are reflected upstream (HR), and particles that

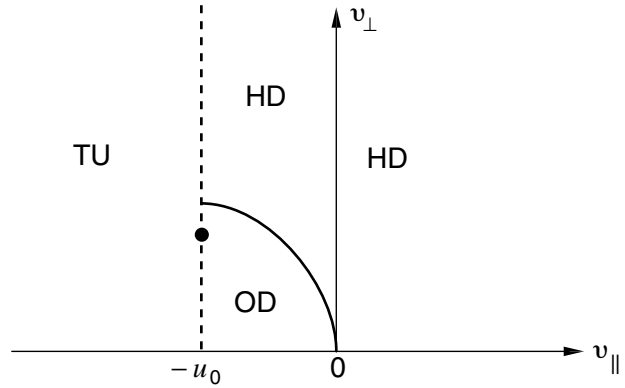


**Figure 4** Schematic of the downstream velocity space in the NIF. The point corresponding to maximum energy gain is indicated by the large dot. The labels on the different regions are explained in the text, and correspond directly to the labels in Figure 3.

have overtaken the shock and been transmitted from downstream to upstream (TU). The subscripts  $i$  for incident and  $r$  for reflected are included to distinguish between particles before and after reflection, respectively. The particles in the regions labelled OR and HR satisfy equation (9).

#### 4.2 The Downstream Velocity Space

A schematic plot of the downstream velocity space is shown in Figure 4. The diagonal lines in Figure 3 map into the vertical line at  $v_{\parallel} = v\mu = -u_0$  in Figure 4. The HD and OD particles in Figure 3 fill the entire region to the right of the vertical dashed line in Figure 4, and the separation between them (the segment of the  $v_{\perp}$ -axis below the intersection with the diagonal line in Figure 3) maps into a curve which is drawn only schematically in Figure 4. The particles to the left of the vertical dashed line in Figure 4 encounter the shock and are transmitted into the upstream region.

### 5 The Energy Change

Although there is no energy change in the dHT frame, in the NIF particles tend to gain energy when reflected from or transmitted through a shock, because the particles drift along the shock in the direction of the electric force. The energy change can be determined by considering the change in the particle momentum in the dHT frame, and then applying the Lorentz transformation to find the change in the NIF. Toptyghin (1980, 1985) presented expressions for the energy change of test particles reflected from or transmitted through a shock. All reflected particles gain energy from the encounter, but some transmitted particles lose energy (Webb, Axford, & Terasawa 1983).

#### 5.1 Reflected Particles

The maximum energy increase is largest for reflected particles. Reflection is possible only when (9) is satisfied, and the interesting case is when  $\tan \psi_1$  is large, i.e. when  $\mathbf{B}$  is nearly parallel to the shock front. Then the momentum component along the  $y$ -axis (the direction of the relative velocity between the two frames) is

approximately equal to the parallel momentum. The Lorentz transformation implies an energy change on reflection equal to  $\Delta\varepsilon = u_0 \Delta p'_y$ , which therefore implies  $\Delta\varepsilon \approx u_0 \Delta(p' \cos \alpha')$ . On reflection  $p' \cos \alpha'$  changes sign, so  $\Delta(p' \cos \alpha') = 2p' \cos \alpha'$ . Then using (4) and (5) to reexpress the result in terms of  $p$  and  $\alpha$ , it follows that the change in energy on reflection is given by

$$(\Delta\varepsilon)_{\text{ref}} = 2\varepsilon \left( \frac{u_1 \tan \psi_1 v}{c^2} \right) \left( \cos \alpha + \frac{u_1 \tan \psi_1}{v} \right). \quad (10)$$

Shock drift acceleration preferentially increases the parallel energy of a reflected particle, and so leads to a decrease in the pitch angle.

The energy ratio  $\varepsilon_r/\varepsilon_i$  of the reflected ( $r$ ) to the incident ( $i$ ) particles follows from (10), subject to the restrictions (4) and (9). However, in the nonrelativistic limit the ratio of the kinetic energies,  $E_r/E_i = v_r^2/v_i^2$ , where  $E = \varepsilon - mc^2$ , is most simply deduced from Figure 3. Consider two points, A =  $(v_{i\parallel}, v_{i\perp})$  and B =  $(v_{r\parallel}, v_{r\perp})$ , that correspond to a particle before and after reflection. Then  $v_{r\perp} = v_{i\perp}$  and  $v_{r\parallel} = -2u_0 - v_{i\parallel}$ , so if A is the point  $v_{i\perp}$ ,  $v_{i\parallel} = -x$  in velocity space, B is the point  $v_{r\perp}$ ,  $v_{r\parallel} = -(2u_0 - x)$ , cf. Figure 6. Thus

$$\frac{E_r}{E_i} = \frac{v_r^2}{v_i^2} = \frac{(2u_0 - x)^2 + v_{\perp}^2}{x^2 + v_{\perp}^2}. \quad (11)$$

A surface plot and contour plot of the energy ratio of the reflected particles, as a function of  $(v_{i\parallel}, v_{i\perp})$ , is shown in Figure 5. The figure shows clearly that the energy ratio is modest, and that only particles from a small region of phase space near the boundary of the region from which reflection occurs attain a significant fraction of the maximum possible energy increase.

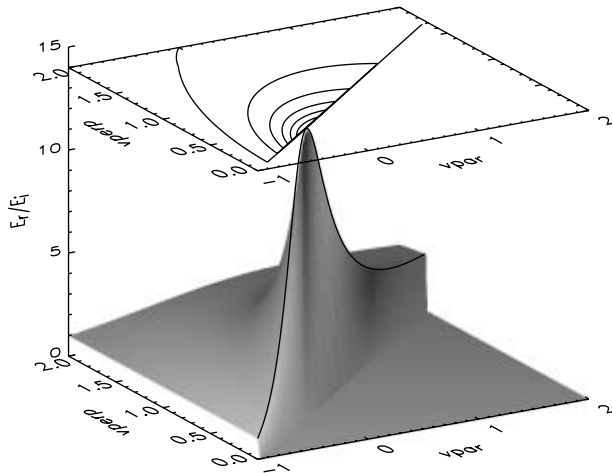


**Figure 5** Energy ratio for particles reflected upstream from a shock with  $B_1/B_2 = 0.25$ , as a function of pre-shock velocity with  $v_{\text{par}} = v_{i\parallel}/u_0$  and  $v_{\text{perp}} = v_{i\perp}/u_0$ . The lowest contour shown corresponds to an energy ratio of 2, and the contour values increase in units of 2.

It is clear from Figure 5 that the maximum value of  $E_r/E_i$  occurs on the slanted line where  $v_{\perp}$  is minimized ( $\alpha' = \alpha_c$ ,  $\sin^2 \alpha_c = B_1/B_2$ ), that separates the region where particles are reflected from the region where they are transmitted, cf. Figure 6. For this case equation (5) implies

$$\begin{aligned} v_{\perp} &= v_i \sin \alpha_i = v_r \sin \alpha_r = (u_0 - x) \tan \alpha_c, \\ v_{i\parallel} &= v_i \cos \alpha_i = -x, \quad v_{r\parallel} = v_r \cos \alpha_r = -(2u_0 - x). \end{aligned} \quad (12)$$

Substitution of (12) into (11) then gives

$$\left. \frac{E_r}{E_i} \right|_{\alpha_c} = \frac{(2u_0 - x)^2 + (u_0 - x)^2 \tan^2 \alpha_c}{x^2 + (u_0 - x)^2 \tan^2 \alpha_c}. \quad (13)$$

The maximum kinetic energy ratio is found by maximizing (13) as a function of  $x$ . It occurs for  $x = x_{\text{max}}$  where

$$x_{\text{max}} = u_0(1 - \cos \alpha_c), \quad (14)$$

and takes the value

$$\left( \frac{E_r}{E_i} \right)_{\text{max}} = \frac{1 + (1 - B_1/B_2)^{1/2}}{1 - (1 - B_1/B_2)^{1/2}}, \quad (15)$$

which also applies to the relativistic case (Kirk 1994). (Earlier suggestions that the maximum energy ratio occurs for the minimum  $v_i$ , which corresponds to  $x = u_0 \sin^2 \alpha_c$  and gives  $\varepsilon_r/\varepsilon_i = (4B_2 - 3B_1)/B_1$ , are incorrect (e.g. Toptyghin 1980).)

The maximum density compression, and magnetic field increase, at a nonrelativistic shock in a fluid with an adiabatic index of 5/3, occurs when the shock is nearly perpendicular. In this case  $B_1/B_2 = 1/4$  and the maximum value of the energy ratio given by equation (15) is

$$\left( \frac{E_r}{E_i} \right)_{\text{max}} = 13.93. \quad (16)$$

To summarise the initial and final properties of the particles which experience the maximum energy gain we introduce the quantity

$$a = \frac{u_0}{v} \quad (17)$$

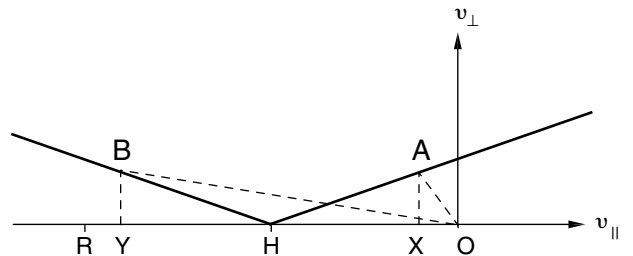


**Figure 6** Velocity space in the NIF: O ( $v_{\parallel} = 0$ ,  $v_{\perp} = 0$ ) is the origin; H ( $v_{\parallel} = -u_0$ ,  $v_{\perp} = 0$ ) is the origin in the dHTF; R ( $v_{\parallel} = -2u_0$ ,  $v_{\perp} = 0$ ) is the reflection of O. The slanted lines are the same as in Figure 3. The point A at  $v_{\parallel} = -x$  and its reflection B at  $v_{\parallel} = -(2u_0 - x)$  are those for which the ratio of the lengths OB to OA, and hence the energy ratio, is maximised.

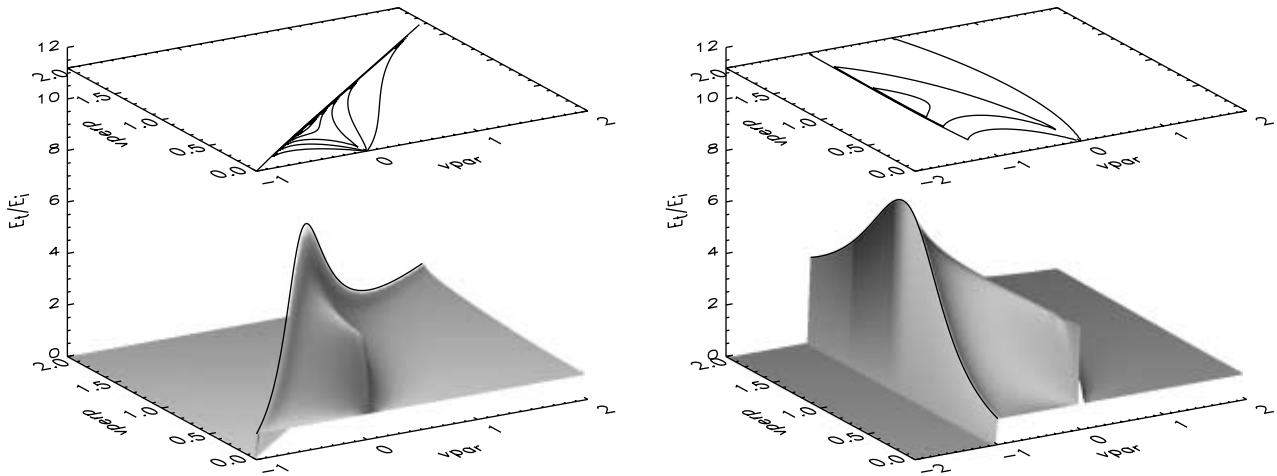


**Figure 7** Energy ratio for particles transmitted from upstream to downstream through a shock with  $B_1/B_2 = 0.25$ , with  $v_{\text{par}} = v_{\parallel}/u_0$  and  $v_{\text{perp}} = v_{\perp}/u_0$ . Left: as a function of pre-shock (upstream) velocity with contours shown corresponding to energy ratio values 1, 2, ..., 6. Right: as a function of post-shock (downstream) velocity with contours shown corresponding to energy ratio values 2, 4 and 6.

and note that the condition for reflection, equation (4), can be written in terms of  $\mu' = \cos \alpha'$  as

$$\mu' < \mu_c \quad \text{where} \quad \mu_c = (1 - b)^{1/2} \quad \text{and} \quad b = \frac{B_1}{B_2}. \quad (18)$$

Then the initial parameters of particles which gain the maximum energy benefit on reflection are

$$a_{i \max} = \left\{ \frac{1}{2b} [1 + (1 - b)^{1/2}] \right\}^{1/2}, \quad (19)$$

$$\mu_{i \max} = - \left\{ \frac{1}{2} [1 - (1 - b)^{1/2}] \right\}^{1/2},$$

and the final parameters of those particles after reflection are

$$a_{r \max} = \left\{ \frac{1}{2b} [1 - (1 - b)^{1/2}] \right\}^{1/2}, \quad (20)$$

$$\mu_{r \max} = - \left\{ \frac{1}{2} [1 + (1 - b)^{1/2}] \right\}^{1/2}.$$

These results correspond to

$$v_i = 2u_0 \sin(\alpha_c/2), \quad v_r = 2u_0 \cos(\alpha_c/2),$$

$$\left( \frac{E_r}{E_i} \right)_{\max} = \cot^2(\alpha_c/2). \quad (21)$$

## 5.2 Transmitted Particles

There are two kinds of transmitted particles: those starting upstream and transmitted downstream, and those starting downstream and transmitted upstream.

### 5.2.1 Upstream to Downstream

For particles transmitted ( $t$ ) from upstream to downstream, in the dHTF one has

$$1 - \mu_t'^2 = b^{-1}(1 - \mu_i'^2), \quad v_t' = v_i'. \quad (22)$$

It is possible to derive the final parameters of the transmitted particles in terms of the initial parameters from equation (22) with (6) and (7). The ratio of the energy of the transmitted particles to the initial (upstream) energy can be written as

$$\frac{E_{td}}{E_{iu}} = \frac{v_{td}^2}{v_{iu}^2}$$

$$= \frac{\left\{ u_0 - [v_{u\perp}^2(1 - b^{-1}) + (v_{u\parallel} + u_0)^2]^{1/2} \right\}^2 + v_{u\perp}^2/b}{v_{u\parallel}^2 + v_{u\perp}^2}, \quad (23)$$

where  $\mathbf{v}_u = \mathbf{v}_i$ , and this ratio is illustrated in Figure 7.

The maximum energy ratio of the transmitted particles is

$$\left( \frac{E_{td}}{E_{iu}} \right)_{\max} = \frac{1}{b} [1 + (1 - b)^{1/2}]. \quad (24)$$

This maximum is attained for the same values of  $a_i$  and  $\mu_i$  as for the maximum energy gain on reflection given by equation (19), and the corresponding values of  $a_t$ ,  $\mu_t$  are

$$a_{t \max} = \frac{1}{2^{1/2}}, \quad \mu_{t \max} = -\frac{1}{2^{1/2}}. \quad (25)$$

Note that the final speed of the transmitted particle at this maximum is independent of the compression ratio,  $v_{t \max} = 2^{1/2}u_0$ . The increase in the energy ratio (24) with decreasing  $b$  (increasing compression ratio) is due to a decrease (with decreasing  $b$ ) in the initial speed,  $v_{i \max} = \{2[1 - (1 - b)^{1/2}]\}^{1/2}u_0$ .

### 5.2.2 Downstream to Upstream

For particles transmitted from downstream to upstream, the energy ratio of the transmitted particles to the initial

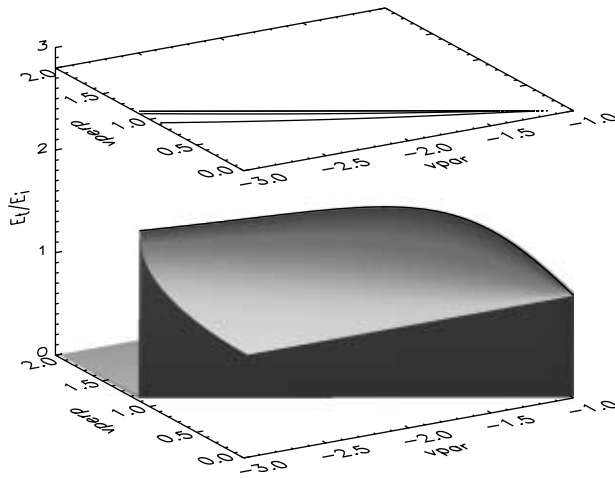


**Figure 8** Energy ratio for particles transmitted from downstream to upstream through a shock with  $B_1/B_2=0.25$ , as a function of post-shock (upstream) velocity with  $v_{\text{par}} = v_{\parallel}/u_0$  and  $v_{\text{perp}} = v_{\perp}/u_0$ . The contours shown correspond to energy ratio values 1.2 and 1.4.

(downstream) energy can be written as

$$\frac{E_{tu}}{E_{id}} = \frac{v_{tu}^2}{v_{id}^2} = \frac{v_{u\parallel}^2 + v_{u\perp}^2}{\left\{u_0 + [v_{u\perp}^2(1-b^{-1}) + (v_{u\parallel} + u_0)^2]^{1/2}\right\}^2 + v_{u\perp}^2/b} \quad (26)$$

where now  $\mathbf{v}_u = \mathbf{v}_f$ , and this ratio is illustrated in Figure 8.

The maximum energy ratio of the particles is

$$\left(\frac{E_{tu}}{E_{id}}\right)_{\text{max}} = 1 + (1-b)^{1/2}, \quad (27)$$

which occurs for particles with initial parameters

$$a_{id} = \frac{1}{2^{1/2}}, \quad \mu_{id} = -\frac{1}{2^{1/2}} \quad (28)$$

which attain parameters

$$a_{tu} = \left\{\frac{1}{2b} [1 - (1-b)^{1/2}]\right\}^{1/2}, \quad (29)$$

$$\mu_{tu} = -\left\{\frac{1}{2} [1 + (1-b)^{1/2}]\right\}^{1/2}.$$

## 6 Structure within the Shock

Although shocks are often modelled as simple discontinuities, the fluid parameters change from their upstream to their downstream values over a finite distance. When the natural length scales of the processes being considered are much greater than the shock thickness the detailed structure of the shock can be ignored. However, when the length scales are comparable to or less than the shock

thickness it is essential to take account of the detailed structure of the shock transition. The thickness of a ‘collisionless’ shock transition is comparable to the gyroradius of the bulk of the ions in the plasma. Energetic ions have much larger gyroradii and so see the shock essentially as a simple discontinuity. Electrons have much smaller gyroradii than ions of comparable energy, so the detailed structure of shock transitions is particularly important for electron processes.

In the dHTF ions incident on the shock from upstream are slowed down and deflected as they cross the shock. The forces responsible arise from a magnetic field component within the shock which is out of the plane of coplanarity of the upstream and downstream fields  $\mathbf{B}'_1$  and  $\mathbf{B}'_2$ , and from an electric field associated with a potential difference,  $\phi'$ , across the shock (e.g. review by Onsager & Thomsen 1991, and references therein). The presence of a component of the magnetic field out of the ‘plane of coplanarity’ (the plane containing the upstream and downstream plasma velocities) was first postulated by Goodrich & Scudder (1984), in order to match the deceleration of the ion plasma flow in the NIF and the dHTF. It was later shown by Jones & Ellison (1987) that the non-coplanar magnetic field is necessary to cancel currents within the plane of coplanarity, which otherwise arise because of the unequal mass of electrons and ions. Jones & Ellison (1987) calculated an expression for the integral of the non-coplanar magnetic field component across the shock layer, but were unable to predict its maximum value. The magnitude of this component has since been estimated from numerical simulations of shock fronts and from observations with spacecraft at the Earth’s bowshock which have detected the non-coplanar field directly, and may be as great as the upstream magnetic field strength  $B_1$  (Thomsen et al. 1987; Gosling, Winske, & Thomsen 1988; Friedman et al. 1990). Also relevant is the observed magnetic ‘overshoot’ — in which the magnitude of the magnetic field is seen to increase beyond  $B_2$  in the shock transition region, before dropping again to  $B_2$  on the downstream side of the shock (Leroy et al. 1982). Thus a particle interacting with the shock front encounters a maximum magnetic field strength  $B_{\text{max}}$  which is somewhat greater than  $B_2$ .

The cross-shock electric field slows down ions, and hence accelerates electrons. The magnetic field structures within the shock increase the maximum magnetic field seen by particles and have the effect of increasing the ‘reflectivity’ of the mirror. The effects of the cross-shock potential on the orbits of individual electrons have been considered in detail for strictly perpendicular shocks (Balikhin, Gedalin, & Petrukovich 1993; Balikhin & Gedalin 1994; Gedalin et al. 1995a; Ball & Galloway 1998), and the treatment generalised to quasi-perpendicular shocks by Gedalin et al. (1995b). Here we consider the modifications of the treatment of shock drift acceleration given above due to these internal shock structures, under the assumption that after averaging over gyrophase the magnetic moment  $p_{\perp}^2/B$  is conserved.

### 6.1 Conditions for Reflection

As electrons cross the shock, conservation of energy in the dHTF requires  $\frac{1}{2}mv^2(x) - e\phi'(x) = \text{constant} = \frac{1}{2}mv_i^2 - e\phi'_i$ , where  $x$  denotes distance through the shock profile. The magnetic moment is also conserved, corresponding to  $v_\perp^2(x)/B(x) = \text{constant} = v_{i\perp}^2/B_i$ . Together these imply

$$v_\parallel^2(x) = v_i^2 - \frac{2e\phi'_i}{m} - v_{i\perp}^2 \frac{B(x)}{B_i} + \frac{2e\phi'(x)}{m}. \quad (30)$$

Particles will be reflected if  $v_\parallel(x) = 0$  (or equivalently, if  $v_\perp^2(x) = v^2(x)$ ) for some value of  $x$  within the shock. In general the details of the magnetic field and electric potential dependence through the shock will be important for determining whether or not a particle is reflected. However, the case where the field increases monotonically from upstream to downstream — i.e. when any magnetic overshoot is neglected — is relatively simple. We first define the following parameters:

$$\phi'_u = 0 \quad \phi'_d = \phi' \quad (31)$$

are the values of the electric potential on the upstream and downstream sides of the shock, respectively, and

$$U = \sqrt{\frac{2e\phi'}{m}} \quad (32)$$

is a constant such that  $\frac{1}{2}mU^2$  is the decrease in the electric potential energy of an electron on crossing the shock from upstream to downstream.

#### 6.1.1 Upstream Reflection, No Magnetic Overshoot

The limiting condition for particles which encounter the shock from upstream ( $v_\parallel > 0$  and  $B_i = B_1$ ,  $\phi'_i = \phi'_u = 0$ ) and are just reflected at the downstream edge of the shock is equivalent to requiring that  $v_\parallel(x) = 0$  for the downstream parameters,  $B(x) = B_2$  and  $2e\phi'(x)/m = U^2$ . It follows from equation (30) that the *limiting boundary* in the upstream dHTF velocity space, such that the particles above the curve are reflected, corresponds to

$$v_{u\perp}^2 = \frac{b}{1-b} (v_{u\parallel}^2 + U^2) \quad (33)$$

with  $b = B_1/B_2$ . The conditions for upstream reflection in the NIF are thus

$$v_{u\parallel} > -u_0, \quad \text{and} \quad v_{u\perp}^2 > \frac{b}{1-b} \left[ (v_{u\parallel} + u_0)^2 + U^2 \right], \quad (34)$$

which implies that there can be no reflected particles with  $v_\perp < v_{\perp \min}$ ,

$$v_{\perp \min} = U \sqrt{\frac{b}{1-b}}. \quad (35)$$

Particles with  $v_{u\perp}^2$  less than that defined by the limiting curve in (34), and with  $v_{u\parallel} > -u_0$ , encounter the shock

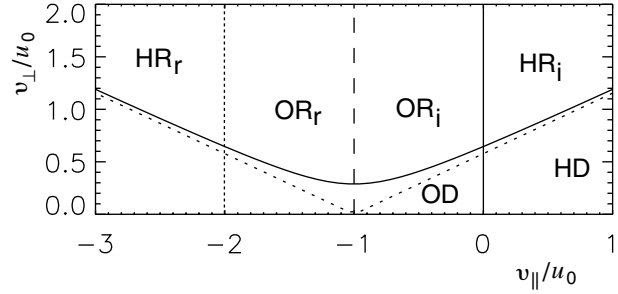


**Figure 9** The upstream phase space in the NIF when a cross-shock potential is included. The labels are explained in Section 4.1 in association with Figure 3. The limiting boundary is the solid curve, which approaches the sloping dotted lines as  $U \rightarrow 0$ . Particles below the limiting boundary (solid line) and to the right of the vertical dashed line at  $v_\parallel = -u_0$  encounter the shock and are transmitted downstream.

and are transmitted from upstream to downstream. Figure 9 illustrates these different regions of the upstream phase space in the NIF.

The geometric argument used to determine the maximum energy ratio on reflection (given above in connection with Figure 6) can be generalised to include the parallel electric field. The energy ratio for a reflected particle is given by equation (11). In place of equation (12) one finds

$$\begin{aligned} v_\perp &= v_i \sin \alpha_i = v_r \sin \alpha_r = [(u_0 - x)^2 + U^2]^{1/2} \tan \alpha_c, \\ v_{i\parallel} &= v_i \cos \alpha_i = -x, \quad v_{r\parallel} = v_r \cos \alpha_r = -(2u_0 - x). \end{aligned} \quad (36)$$

The energy ratio on the limiting boundary is then

$$\frac{E_r}{E_i \text{ limit}} = \frac{(2u_0 - x)^2 + [(u_0 - x)^2 + U^2] \tan^2 \alpha_c}{x^2 + [(u_0 - x)^2 + U^2] \tan^2 \alpha_c}, \quad (37)$$

which has zero derivative when

$$\begin{aligned} [(u_0 - x)^2 + U^2] \tan^2 \alpha_c &= x(2u_0 - x), \quad \text{or} \\ x^2 - 2u_0x + (u_0^2 - U^2) \sin^2 \alpha_c &= 0. \end{aligned} \quad (38)$$

Writing the solutions as  $x = x_\pm$ , one finds

$$x_\pm = u_0 \pm (u_0^2 \cos^2 \alpha_c + U^2 \sin^2 \alpha_c)^{1/2}, \quad (39)$$

which correspond to

$$v_i^2 = 2u_0x_- + U^2 \sin^2 \alpha_c, \quad v_r^2 = 2u_0x_+ + U^2 \sin^2 \alpha_c, \quad (40)$$

whence

$$\left( \frac{E_r}{E_i} \right)_{\max} = \frac{2u_0^2 + 2u_0 (u_0^2 \cos^2 \alpha_c + U^2 \sin^2 \alpha_c)^{1/2} + U^2 \sin^2 \alpha_c}{2u_0^2 - 2u_0 (u_0^2 \cos^2 \alpha_c + U^2 \sin^2 \alpha_c)^{1/2} + U^2 \sin^2 \alpha_c}. \quad (41)$$

Note that (41) implies that the maximum energy ratio is an increasing function of  $U^2$ .

### 6.1.2 Downstream Reflection, No Magnetic Overshoot

When the cross-shock potential is included it is also possible for particles which encounter the shock from downstream to be reflected. By direct analogy with reflection from upstream, the conditions for reflection are as follows. Only particles with  $v'_{\parallel} < 0$  in the downstream region can encounter the shock. The condition for reflection of such particles ( $B_i = B_2$ ,  $\phi'_i = \phi'_d = \phi'$ ) at the upstream edge of the shock is that  $v'_{\parallel}(x) = 0$  for the upstream parameters,  $B(x) = B_1$  and  $2e\phi'(x)/m = 0$ . It then follows from equation (30) that the limiting boundary in the downstream dHTF, such that particles below the curve are reflected downstream, is

$$v_{d\perp}^2 = \frac{1}{1-b} (-v_{d\parallel}^2 + U^2). \quad (42)$$

When  $v'_{d\parallel} < -U$  the right hand side of equation (42) is negative and particles cannot be reflected. The conditions for downstream reflection in the NIF are thus

$$-U - u_0 < v_{d\parallel} < -u_0, \quad \text{and} \\ v_{d\perp}^2 < \frac{1}{1-b} [-(v_{d\parallel} + u_0)^2 + U^2]. \quad (43)$$

All particles with  $v_{d\parallel} < -U - u_0$ , and particles with  $-U - u_0 < v_{d\parallel} < -u_0$  and  $v_{d\perp}^2$  greater than that defined by the limiting curve in (43), will encounter the shock and be transmitted from downstream to upstream. Figure 10 illustrates these different regions of the downstream phase space in the NIF.

### 6.1.3 Upstream and Downstream Reflection, with Magnetic Overshoot

In the simplest treatment including both a magnetic overshoot and a cross-shock potential, the condition for particles to be reflected upstream is straightforward. If the maximum magnetic field is  $B_{\max}$ , then the limiting

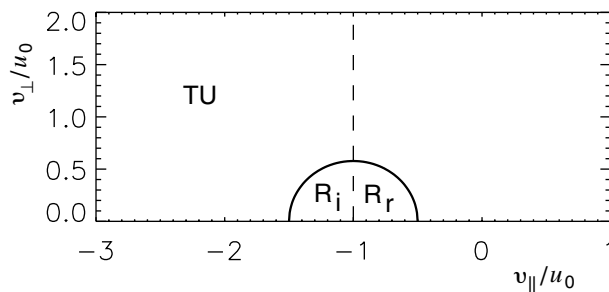


**Figure 10** The downstream phase space in the NIF showing the limiting boundary — the solid ellipse — when there is a cross-shock potential (with  $U = u_0/2$ ) but no magnetic overshoot ( $b = b_{m1} = 0.25$ ). Particles to the left of the vertical dashed line at  $v_{\parallel} = -u_0$  encounter the shock. Of these, the particles which are also below the limiting boundary — i.e. in the region labelled  $R_i$  — are reflected and appear in the region labelled  $R_r$ . Particles to the left of the vertical dashed line and above the limiting boundary — i.e. in the region labelled TU — are transmitted from downstream to upstream.

boundary in the upstream NIF is simply given by equation (34) with  $b$  replaced by the parameter  $b_{m1} = B_1/B_{\max}$  which satisfies  $b_{m1} < b$ . Since the maximum magnetic field which can reflect the particles is higher than when there is no overshoot, the region of phase space from which particles can be reflected upstream is larger. In particular, the minimum value of  $v_{u\perp}$  for which particles can be reflected is larger, and the slope of the limiting boundary at large  $|v'_{u\parallel}|$ , namely  $\sqrt{b_{m1}/(1-b_{m1})}$ , is smaller.

The inclusion of a magnetic overshoot implies that particles incident on the shock from downstream can also be reflected, even when the cross-shock potential is zero. This arises because of the magnetic mirror associated with the fact that the maximum magnetic field is greater than the downstream field, and it results in a qualitative change in the limiting boundary. In this case the conditions for downstream reflection in the NIF are

$$v_{d\parallel} < -u_0, \quad \text{and} \\ v_{d\perp}^2 > \frac{b_{m2}}{1-b_{m2}} [(v_{d\parallel} + u_0)^2 - U^2] \quad (44)$$

where  $b_{m2} = B_2/B_{\max} = b_{m1}/b$ . Note that when  $-U - u_0 < v_{d\parallel} < -u_0$  the right hand side of equation (44) is negative, and so all such particles are reflected. Figure 11 illustrates these different regions in the downstream phase space in the NIF.

### 6.1.4 Transmitted Particles

We now consider the fate of the particles which are transmitted through the shock.

Particles initially upstream of the shock which satisfy the conditions

$$v_{u\parallel} > -u_0, \quad \text{and} \\ v_{u\perp}^2 < \frac{b_{m1}}{1-b_{m1}} [(v_{u\parallel} + u_0)^2 + U^2], \quad (45)$$

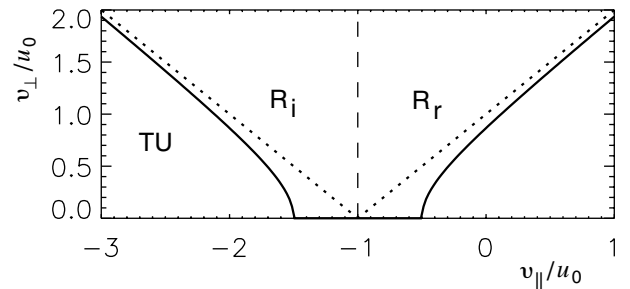


**Figure 11** The downstream phase space in the NIF when there is a magnetic overshoot (with  $b = 0.25$  and  $b_{m2} = 0.5$ ). The solid curves are the limiting boundary when there is also a cross-shock potential (with  $U = u_0/2$ ) and the dotted lines show the boundary when  $U = 0$ . Particles to the left of the vertical dashed line at  $v_{\parallel} = -u_0$  encounter the shock. Of these, particles above the limiting boundary — i.e. in the region labelled  $R_i$  — are reflected downstream and appear in the region labelled  $R_r$ . Particles to the left of the vertical dashed line and below the limiting boundary — labelled TU — are transmitted from downstream to upstream.

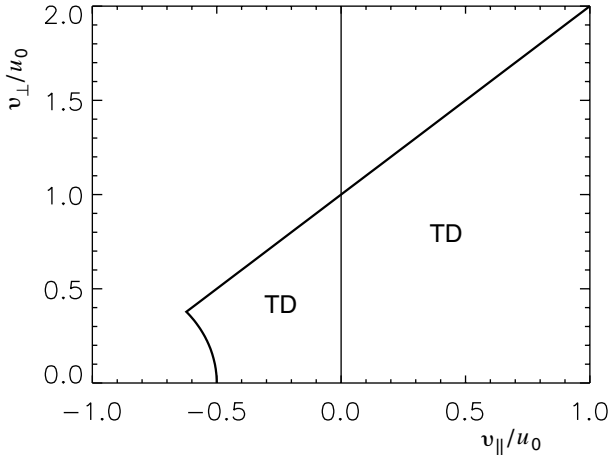


**Figure 12** The downstream phase space in the NIF, showing the region occupied by electrons transmitted from upstream to downstream, when there is a magnetic overshoot and a cross-shock potential (with  $b = 0.25$ ,  $b_{m1} = 0.125$  and  $U = u_0/2$ ).

are transmitted from upstream to downstream (cf. equation (34)). After transmission the particles have velocities

$$\begin{aligned} v_{d\perp}^2 &= b^{-1}v_{u\perp}^2, \\ v_{d\parallel} &= (v_u^2 + 2u_0v_{u\parallel} - b^{-1}v_{u\perp}^2 + u_0^2 + U^2)^{1/2} - u_0, \end{aligned} \quad (46)$$

with  $b = B_1/B_2 \geq b_{m1} = B_1/B_{\max}$ . The boundary of the region of downstream phase space occupied by the transmitted particles comprises part of an ellipse together with a straight line, as shown in Figure 12. The ellipse is the boundary of the region

$$\begin{aligned} 0 \leq v_{d\perp} \leq U \sqrt{\frac{b_{m1}}{b(1-b_{m1})}}, \quad \text{and} \\ v_{d\parallel} \geq [v_{d\perp}^2(b-1) + U^2]^{1/2} - u_0, \end{aligned} \quad (47)$$

and the straight line bounds the region

$$\begin{aligned} v_{d\perp} \geq U \sqrt{\frac{b_{m1}}{b(1-b_{m1})}}, \quad \text{and} \\ v_{d\parallel} \geq v_{d\perp} \left[ \frac{b(1-b_{m1})}{b_{m1}} + b - 1 \right]^{1/2} - u_0. \end{aligned} \quad (48)$$

When there is a cross-shock potential but no magnetic overshoot, electrons initially downstream of the shock which satisfy the conditions

$$\begin{aligned} v_{d\parallel} < -u_0, \quad \text{and} \\ v_{d\perp}^2 > \frac{1}{1-b} [-(v_{d\parallel} + u_0)^2 + U^2], \end{aligned} \quad (49)$$

are transmitted from downstream to upstream. After transmission the electrons have velocities

$$\begin{aligned} v_{u\perp}^2 &= bv_{d\perp}^2, \\ v_{u\parallel} &= -(v_d^2 + 2u_0v_{d\parallel} - bv_{d\perp}^2 + u_0^2 - U^2)^{1/2} - u_0. \end{aligned} \quad (50)$$

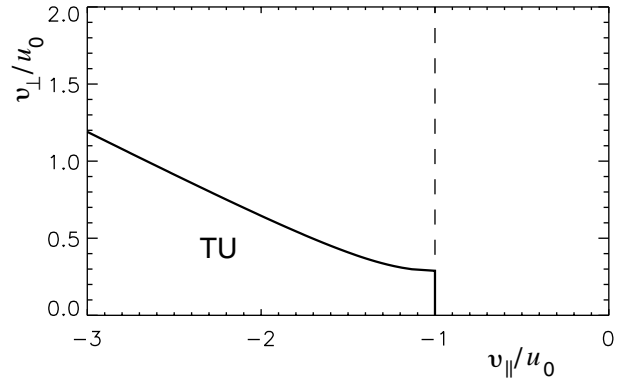


**Figure 13** The upstream phase space in the NIF, showing the region occupied by electrons transmitted from downstream to upstream, when there is a cross-shock potential (with  $U = u_0/2$ ) but no magnetic overshoot (with  $b = b_{m1} = 0.25$ ).

The boundary of the region occupied by the transmitted electrons in the upstream phase space is shown in Figure 13. The vertical straight line bounds the region

$$\begin{aligned} v_{u\perp} < U \sqrt{\frac{b}{1-b}}, \quad \text{and} \\ v_{u\parallel} < -u_0, \end{aligned} \quad (51)$$

and the curve bounds the region

$$\begin{aligned} v_{u\perp} > U \sqrt{\frac{b}{1-b}}, \quad \text{and} \\ v_{u\parallel} < - \left[ v_{u\perp}^2 \frac{(1-b)}{b} - U^2 \right]^{1/2} - u_0. \end{aligned} \quad (52)$$

When there is both a cross-shock potential and a magnetic overshoot the boundary of the region of phase space occupied by electrons transmitted from downstream to upstream is simpler. Electrons which satisfy

$$\begin{aligned} v_{d\parallel} < -U - u_0, \quad \text{and} \\ v_{d\perp}^2 < \frac{b_{m2}}{1-b_{m2}} [(v_{d\parallel} + u_0)^2 - U^2] \end{aligned} \quad (53)$$

are transmitted. They occupy the region of upstream phase space bounded by the straight line

$$v_{u\parallel} < -v_{u\perp} \left( \frac{1-bb_{m2}}{bb_{m2}} \right)^{1/2} - u_0. \quad (54)$$

### 6.1.5 Forbidden and Overlap Regions

When there is no magnetic overshoot in the shock the boundaries of the regions of phase space occupied by reflected and transmitted electrons are the same. When there is a magnetic overshoot the boundaries can be different, and there can be ‘forbidden regions’ of phase space in which electrons can never encounter the shock, and ‘overlap regions’ in which electrons may have been either transmitted through or reflected from the shock.

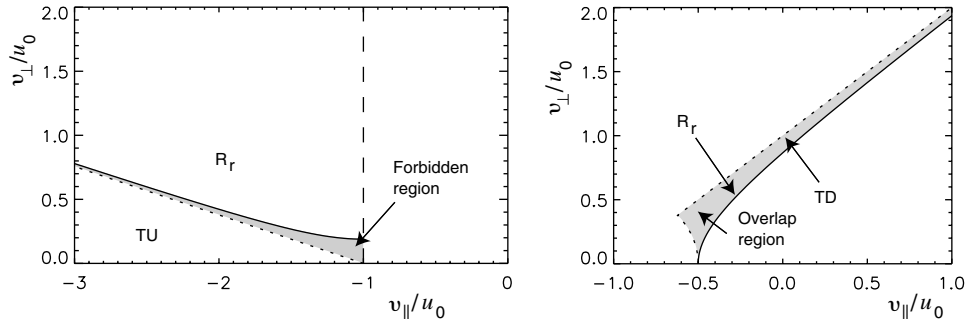


**Figure 14** Left: the upstream phase space in the NIF, showing the forbidden region occupied by electrons which can never encounter the shock. Right: the downstream phase space in the NIF, showing the overlap region occupied by electrons reflected downstream and by electrons transmitted from upstream to downstream. The parameters used here are  $b = 0.25$ ,  $b_{m1} = 0.125$  and  $U = u_0/2$ .

In the half-plane of the upstream phase space with  $v_{u\parallel} < -u_0$ , there is a forbidden region which is not accessible to electrons which have been reflected upstream or those which have been transmitted from downstream to upstream. In the half-plane of the downstream phase space with  $v_{d\parallel} > -u_0$ , there is an overlap region populated both by electrons which have been reflected downstream and those which have been transmitted from upstream to downstream.

These regions are illustrated in Figure 14. In the upstream phase space, electrons reflected from the shock ( $R_r$ ) occupy the region to the left of the vertical dashed line and above the solid curve. Electrons transmitted from downstream to upstream (TU) lie below the dotted sloping line. The shaded region is forbidden in the sense that electrons between the dotted and solid boundaries never encounter the shock. In the downstream phase space, electrons reflected from the shock ( $R_r$ ) occupy the region above the solid curve. Electrons transmitted from upstream to downstream (TD) lie below the dotted boundary. In the shaded overlap region these two populations coexist.

Studies of the population of electrons around the forbidden region at the Earth's bow shock indicate that electrons may indeed avoid the forbidden region (Feldman 1985; Scudder et al. 1986; Gosling et al. 1989), which may provide support for arguments that shock drift acceleration operates at collisionless shocks in the heliosphere.

## 7 Effectiveness of Acceleration

In order for shock drift acceleration to be an important effect in physical systems, a significant fraction of the electrons incident on the shock must experience a substantial energy gain. In this section we seek to quantify this requirement.

### 7.1 The Parallel Distribution Function

Let  $f_i(v_{i\parallel}, v_{\perp})$  be the distribution function of the incident particles, and  $f_r(v_{r\parallel}, v_{\perp})$  be that of the reflected particles. On reflection one has  $v_{r\parallel} = -(2u_0 + v_{i\parallel})$ ; the perpendicular speed is unchanged on reflection, and  $v_{r\perp} = v_{i\perp}$  is denoted  $v_{\perp}$ . It is convenient to define a parallel distribution

function by writing

$$F_i(v_{\parallel}) = 2\pi \int_0^{\infty} dv_{\perp} v_{\perp} f_i(v_{\parallel}, v_{\perp}). \quad (55)$$

For the reflected particles the perpendicular velocity must exceed the limit defined by (34). Writing this condition as

$$v_{\perp}^2 \gtrsim v_{\perp \min}^2 = \frac{b}{1-b} [(v_{\parallel} + u_0)^2 + U^2], \quad (56)$$

one has

$$F_r(v_{\parallel}) = 2\pi \int_{v_{\perp \min}}^{\infty} dv_{\perp} v_{\perp} f_r(v_{\parallel}, v_{\perp}), \quad (57)$$

with

$$f_r(v_{\parallel}, v_{\perp}) = f_i(-2u_0 - v_{\parallel}, v_{\perp}). \quad (58)$$

For an isotropic distribution of incident particles, it is convenient to define

$$G(x) = 2\pi \int_x^{\infty} dv v f_i(v). \quad (59)$$

Then for the incident particles one has  $F_i(v_{i\parallel}) = G(v_{i\parallel})$ . Equation (57) implies that for the particles that are to be reflected by the shock,  $F_r(v_{i\parallel}) = G[(v_{i\parallel}^2 + v_{\perp \min}^2)^{1/2}]$ , before those particles encounter the shock.

#### 7.1.1 Fraction of Reflected Particles

Particles gain energy on reflection, and in considering the efficiency of the acceleration it seems appropriate to consider the conditions under which the number of reflected particles is maximised. The fraction,  $R_r(v_{i\parallel})$ , of the particles reflected is

$$R_r(v_{i\parallel}) = \frac{G(v_i)}{G(v_{i\parallel})}, \quad (60)$$

with  $v_i = (v_{i\parallel}^2 + v_{\perp \min}^2)^{1/2}$  located on the limiting boundary, cf. Figure 9.

According to (60), the fraction of particles reflected is a monotonically decreasing function of increasing  $v_{\perp \min}^2$ . It then follows from (57) that the maximum fraction

reflected occurs for  $v_{i\parallel} = -u_0$ , and from (55) this maximum is

$$(R_r)_{\max} = R_r(-u_0) = \frac{G \left[ (u_0^2 + bU^2/(1-b))^{1/2} \right]}{G(u_0)}, \quad (61)$$

$$U^2 = 2e\phi'/m.$$

However, equation (37) implies that for  $v_{i\parallel} = -u_0$  there is zero energy change on reflection. Thus, it turns out that maximising the fraction of particles reflected is of no relevance to optimising the effectiveness of acceleration.

### 7.1.2 Fraction Reflected with Maximum Energy Change

More relevant in considering the effectiveness of acceleration is the fraction of particles reflected at the value of  $v_{i\parallel}$  where the energy change is maximised. In the absence of a cross-shock potential the relevant particle parameters are given by (12) with (14), or (21). In this case, one has the following values in (60):

$$v_i = 2u_0 \sin(\alpha_c/2), \quad v_{i\parallel} = -2u_0 \sin^2(\alpha_c/2). \quad (62)$$

When the parallel electric field is included, according to (40) with (39), (62) is replaced by

$$v_i^2 = [x_-^2 + u_0 \sin^2(\alpha_c/2)]^{1/2}, \quad v_{i\parallel} = -x_-,$$

$$x_- = u_0 - (u_0^2 \cos^2 \alpha_c + U^2 \sin^2 \alpha_c)^{1/2}. \quad (63)$$

To progress further we need to assume an explicit form for the distribution function. We consider Maxwellian and power law distributions.

### 7.2 Maxwellian Distribution Function

For a Maxwellian distribution,

$$f(v) = \frac{n_e}{(2\pi)^{3/2} V_e^3} \exp\left(-\frac{v^2}{2V_e^2}\right), \quad (64)$$

one has

$$G(v_{\parallel}) = \frac{n_e}{(2\pi)^{1/2} V_e} \exp\left(-\frac{v_{\parallel}^2}{2V_e^2}\right). \quad (65)$$

In this case substitution of either (62) or (63) into (60) implies that the ratio of particles reflected at the value of  $v_{i\parallel}$  where the energy change is maximised, is given by

$$(R_r)_{\text{opt}} = \exp\left(-\frac{v_i^2 - v_{i\parallel}^2}{2V_e^2}\right) = \exp\left(-\frac{u_0^2 \sin^2(\alpha_c/2)}{2V_e^2}\right). \quad (66)$$

The ratio (66) is of order unity for  $u_0^2 \sin^2(\alpha_c/2) \lesssim 2V_e^2$  and is very small when this inequality is strongly reversed. This reflects the fact that for a significant fraction of the initial electrons to be accelerated,  $v_i$  must not be too much greater than the mean thermal speed.

The ratio of the final to the initial energy is  $\cot^2(\alpha_c/2)$ , cf. (21). Hence, one may conclude that for a Maxwellian distribution, SDA can be effective in increasing the energy of electrons with an initial energy of at most a few times the thermal energy by a factor  $\cot^2(\alpha_c/2)$ . For a significant fraction of the thermal electrons to be accelerated requires  $u_0^2 \sin^2(\alpha_c/2) \lesssim 2V_e^2$ .

### 7.3 Power Law Distribution

For particles with a power law distribution of the form

$$f(v) \propto v^{-(\delta+2)}, \quad (67)$$

it follows that

$$G(v_{\parallel}) \propto v_{\parallel}^{-\delta}. \quad (68)$$

Then using (63) one has

$$(R_r)_{\text{opt}} = \left(\frac{v_i}{v_{i\parallel}}\right)^{-\delta} = \left(\frac{x_-^2 + u_0 \sin^2(\alpha_c/2)}{x_-^2}\right)^{-\delta/2}. \quad (69)$$

When the parallel electric field is neglected, (69) simplifies to

$$(R_r)_{\text{opt}} = \sin^{\delta}(\alpha_c/2). \quad (70)$$

The effectiveness of the acceleration in this case may be estimated by comparing the parallel distribution function of the reflected electrons with the electrons at the same  $v_{\parallel}$  in the initial distribution. Taking account of the fraction (70) that are reflected, this ratio is

$$\frac{F_r(v_{r\parallel})}{F_i(v_{r\parallel})} = \sin^{\delta}(\alpha_c/2) (v_{i\parallel}/v_{r\parallel})^{-\delta}$$

$$= \cos^{2\delta}(\alpha_c/2) \sin^{-\delta}(\alpha_c/2). \quad (71)$$

By way of illustration, for  $b=1/2, 1/3, 1/4$ , one has  $\alpha_c = 45^\circ, 35^\circ, 30^\circ$ , and  $\cos^2(\alpha_c/2)/\sin(\alpha_c/2) = 2.23, 3.02, 3.60$ , respectively, and the ratio (71) is given by these final numbers to the power  $\delta$ .

### 7.4 Streaming Instability Criterion

The criterion for growth of Langmuir waves propagating along the magnetic field lines is  $k_{\parallel} dF(v_{\parallel})/dv_{\parallel} > 0$ . One finds

$$\frac{dF(v_{\parallel})}{dv_{\parallel}} = \frac{dG(v_0)}{dv_{\parallel}},$$

$$v_0^2 = \frac{b}{1-b} [(v_{\parallel} + u_0)^2 + U^2] + (v_{\parallel} + 2u_0)^2. \quad (72)$$

The criterion for instability becomes

$$\frac{dv_0^2}{dv_{\parallel}} = 2\frac{b}{1-b}(v_{\parallel} + u_0) + 2(v_{\parallel} + 2u_0) < 0, \quad (73)$$

which reduces to  $v_{\parallel} < -(2-b)u_0$ . One finds

$$\frac{dF(v_{\parallel})}{dv_{\parallel}} = -2\pi G(v_0) \left[ \frac{b}{1-b}(v_{\parallel} + u_0) + (v_{\parallel} + 2u_0) \right], \quad (74)$$

with  $v_0$  given by (72). It is notable that the criterion for growth for an isotropic initial distribution of electrons is independent of the distribution function. However, the magnitude of the growth rate does depend on the details of the distribution function through  $G(v_0)$ .

## 8 Discussion and Conclusions

Our purpose in this paper is to review and extend the known results on shock drift acceleration, especially of nonrelativistic electrons. In one sense, shock drift acceleration is a simple process in that it can be described essentially ballistically by considering reflection and transmission from a shock in the dHTE, and by then transforming to the frame of interest. However, the results are far from simple due to the energy change being substantial only in very restricted ranges of parameter space. In particular, shock drift acceleration causes a substantial change in the energy of particles only in a very localised region of velocity space, as illustrated in Figure 5, and only for a small range of angles between the shock normal and the direction of the magnetic field. We determine the maximum value of the ratio of the final to the initial energy, and find that it has the same value, cf. (15) and (16), as in the relativistic case (Kirk 1994), rather than the value quoted by Toptyghin (1980).

We include the effect of a cross-shock electric field and of the magnetic overshoot, both of which are accepted features in the theory of collisionless shocks. The cross-shock electric field is described by a potential energy  $\frac{1}{2}mU^2$ , and it is found that the ratio of the final to the initial energy of reflected electrons is a monotonically increasing function of  $U^2$ . The magnetic overshoot leads to a forbidden region in the upstream velocity space, and an overlap region in the downstream velocity space which particles can reach in two distinct ways. We also estimate the efficiency of the acceleration by comparing the distributions of incident and reflected particles. However, the sensitivity to the parameters precludes any simple general conclusions relating to the efficiency of shock drift acceleration.

An important suggested application of shock drift acceleration is to the acceleration of electrons that produce Type II solar radio bursts in the solar corona and the solar wind (Holman & Pesses 1983; Leroy & Mangeney 1984; Wu 1984; Street, Ball, & Melrose 1994; Krauss-Varban & Wu 1989). In this context it is important to determine the condition under which the reflected accelerated electrons drive a beam instability, which is assumed to be an essential step in the generation of the radio emission. We show that, for isotropic incident electrons, the condition for the beam instability to develop is independent of the form of the distribution function, and is given by (73). This provides a potential test for the suggestion that shock drift acceleration causes Type II radio emission. We propose to pursue this point in detail elsewhere.

## Acknowledgments

Some of the material presented here builds on the work of Arthur Street conducted during his Honours year. We

thank Peter Dawson who produced the plots of the energy increase as a function of the particle parameters in the course of an RCFTA Vacation Scholarship.

## References

- Armstrong, T. P., & Krimigis, S. M. 1976, *J. Geophys. Res.*, 81, 677  
 Armstrong, T. P., Pesses, M. E., & Decker, R. B. 1985, in *Collisionless Shocks in the Heliosphere: Reviews of Current Research*, eds B. T. Tsurutani, & R. G. Stone (Washington, DC: American Geophysical Union), 271  
 Balikhin, M., & Gedalin, M. 1994, *Geophys. Res. Lett.*, 21, 841  
 Balikhin, M., Gedalin, M., & Petrukovich, A. 1993, *Phys. Rev. Lett.*, 70, 1259  
 Ball, L., & Galloway, D. 1998, *J. Geophys. Res.*, 103, 17455  
 Cairns, I. H. 1986, *PASA*, 6, 444  
 Cairns, I. H. 1987, *J. Geophys. Res.*, 92, 2315  
 de Hoffmann, F., & Teller, E. 1950, *Phys. Rev.*, 80, 692  
 Decker, R. B. 1988, *Space Sc. Rev.*, 48, 195  
 Drury, L. O'C. 1983, *Rep. Prog. Phys.*, 46, 973  
 Feldman, W. C. 1985, *Geophys. Monogr. Ser.*, 35, 195  
 Filbert, P. C., & Kellogg, P. J. 1979, *J. Geophys. Res.*, 84, 1369  
 Fitzenreiter, R. J., Scudder, J. D., & Klimas, A. J. 1990, *J. Geophys. Res.*, 95, 4155  
 Friedman, M. A., Russell, C. T., Gosling, J. T., & Thomsen, M. F. 1990, *J. Geophys. Res.*, 95, 2441  
 Gedalin, M., Gedalin, K., Balikhin, M., & Krasnoselkikh, V. 1995a, *J. Geophys. Res.*, 100, 9481  
 Gedalin, M., Gedalin, K., Balikhin, M., Krasnoselkikh, V., & Wooliscroft, L. J. C. 1995b, *J. Geophys. Res.*, 100, 19911  
 Goodrich, C. C., & Scudder, J. D. 1984, *J. Geophys. Res.*, 89, 6654  
 Gosling, J. T., Winske, D., & Thomsen, M. F. 1988, *J. Geophys. Res.*, 93, 2735  
 Gosling, J. T., Thomsen, M. F., Bame, S. J., & Russell, C. T. 1989, *J. Geophys. Res.*, 94, 10011  
 Holman, G. D., & Pesses, M. E. 1983, *ApJ*, 267, 837  
 Jones, F. C., & Ellison, D. C. 1987, *J. Geophys. Res.*, 92, 11205  
 Kirk, J. G. 1994, in *Kinetic Plasma Physics*, J. G. Kirk, D. B. Melrose, & E. R. Priest (Berlin: Springer-Verlag), 244  
 Kirk, J. G., & Heavens, A. F. 1989, *MNRAS*, 239, 995  
 Krauss-Varban, D., & Wu, C. S. 1989, *J. Geophys. Res.*, 94, 15367  
 Leroy, M. M., & Mangeney, A. 1984, *Annales Geophysicae*, 2, 449  
 Leroy, M. M., Winske, D., Goodrich, C. C., Wu, C. S., & Papadopoulos, K. 1982, *J. Geophys. Res.*, 87, 5081  
 Lopate, C. 1989, *J. Geophys. Res.*, 94, 9995  
 Melrose, D. B. 1994, *ApJS*, 90, 623  
 Onsager, T. G., & Thomsen, M. F. 1991, *Rev. Geophys. Suppl.*, 998  
 Pesses, M. E. 1981, *J. Geophys. Res.*, 86, 150  
 Pesses, M. E., Decker, R. B., & Armstrong, T. P. 1982, *Space Sc. Rev.*, 32, 185  
 Potter, D. W. 1981, *J. Geophys. Res.*, 86, 11111  
 Sarris, E. T., & Krimigis, S. M. 1985, *ApJ*, 298, 676  
 Scudder, J. D., Mangeney, A., Lacombe, C., Harvey, C. C., Wu, C. S., & Anderson, R. R. 1986, *J. Geophys. Res.*, 91, 11075  
 Sonnerup, B. U. O. 1969, *J. Geophys. Res.*, 74, 1301  
 Street, A. G., Ball, L., & Melrose, D. B. 1994, *PASA*, 11, 21  
 Terasawa, T. 1979, *Planet. Sp. Sc.*, 27, 193  
 Thomsen, M. F., Gosling, J. T., Bame, S. J., Quest, K. B., Winske, D., Livesey, W. A., & Russell, C. T. 1987, *J. Geophys. Res.*, 92, 2305  
 Toptyghin, I. N. 1980, *Space Sc. Rev.*, 26, 157  
 Toptyghin, I. N. 1985, *Cosmic Rays in Interplanetary Magnetic Fields*, (Dordrecht: Reidel)  
 Webb, G. M., Axford, W. I., & Terasawa, T. 1983, *ApJ*, 270, 537  
 Wu, C. S. 1984, *J. Geophys. Res.*, 89, 8857  
 Zank, G., & Gaisser, T. K. 1992, *AIP Conf. Proc.*, 264, 509